Local nanofiller volume concentration effect on elastic properties of polymer nanocomposites

Hyunseong Shin, Jin-Gyu Han, Seongmin Chang and Maenghyo Cho[*]

Department of Mechanical and Aerospace Engineering, Seoul National University, San 56-1, Shillim-Dong, Kwanak-Ku, Seoul 151-742, Republic of Korea

Abstract. In this study, an influence of local variation of nanoparticulate volume fraction on the homogenized elastic properties is investigated. It is well known that interface effect is dependent on the radius and volume fraction of reinforced nanofillers. However, there is no study on the multiscale modeling and analysis of polymer nanocomposites including polydispersed nanoparticles with consideration of interphase zone, which is dependent on the volume fraction of corresponding nanoparticles. As results of numerical examples, it is confirmed that an influence of local variation of nanoparticulate volume fraction should be considered for non-dilute system such as cluster of nanoparticles. Therefore representative volume element analysis is conducted by considering local variation of nanoparticle volume fraction in order to analyze the practical size of cell including hundreds of nanoparticles. It is expected that this study could be extended to the multiparticulate nanocomposite systems including polydispersed nanoparticles.

1. Introduction

Polymer-based nanoparticulate composites have been widely used due to their extraordinary properties derived from highly dense adsorption layer around nanoparticles (Thostenson *et al*. 2005, and Zeng *et al*. 2008). High nonbond interaction between reinforced filler and host material changes the arrangement of polymer chains near the nanoparticles (Wei *et al*. 2002). Entangled polymer chains show non-negligible crystallinity and condensed adsorption layer, which constitutes interphase (Yang *et al*. 2012). Structural formation of interphase is primarily dependent on the corresponding particulate radius and distance between adjacent nanoparticles (Yang and Cho 2008, Yang and Cho 2009, Cho *et al*. 2011). It is an indisputable fact that the link between microscopic molecular structure and macroscopic properties provides useful guideline to design and manufacture of nanocomposites. In this regard, multiscale modeling and analysis are a major issue in the field of design and analysis of polymer nanocomposites.

The full-atomistic molecular dynamics (MD) simulation is useful to obtain mechanical response of polymeric nanocomposites. The MD simulation could investigate size effects and

---

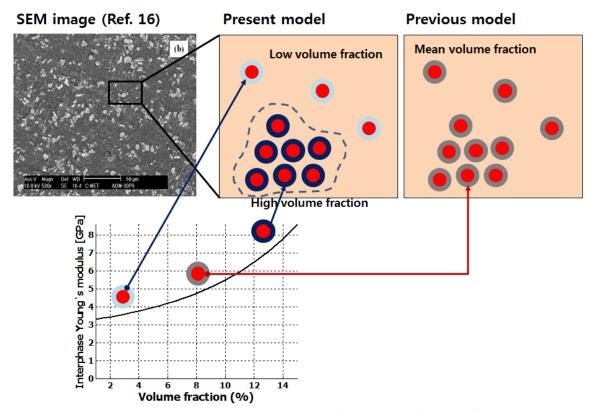*Corresponding author, Professor, E-mail: mhcho@snu.ac.kr

Fig. 1 Motivation of this study: investigation of influence of local volume fraction effect on homogenized elastic properties

volume fraction effects of reinforced fillers embedded in the host polymer matrix with considering chemical treatments such as surface oxidation of nanoparticles, grafting between polymer chain and surface of nanoparticles (Yang *et al*. 2012), and crosslinking network of polymer chains (Kim *et al*. 2015). In MD simulation, formation of interphase zone in the vicinity of nanoparticles are validated due to high nonbond interaction which stems from van der Waals interaction and electrostatic interaction. In order to identify interphase zone of nanocomposites, a number of multiscale modeling strategies are proposed (Yang and Cho 2008, Yang and Cho 2009, Cho *et al*. 2011, and Odegard *et al*. 2005). Among them, Odegard *et al*. (2005) proposed equivalent micromechanics model including effective interface to include nanomechanical response obtained from MD simulation. Yang and Cho (2009) shows that the effective interface is dependent on the particulate size and volume fraction. However, Eshelby's solution-based multiscale modeling strategy is not useful to analyze polydisperse state of multiparticulate nanocomposite systems. To overcome this limitation, Cho *et al*. (2011) proposed multiscale modeling strategy combining multiscale homogenization method with nanomechanical information obtained from MD simulation.

   Meanwhile, uniform size distribution of nanofillers is almost impossible because there is particulate growth. Moreover, filler dispersion is wayward issue in manufacture of polymeric nanocomposites (Xu *et al*. 2012, Liu J *et al*. 2011, and Goyal *et al*. 2008). Therefore, there are

significant local variations of filler volume fraction due to the limitation of manufactures. In this regard, an influence of local volume fraction effect on the homogenized mechanical properties of overall system is important issue as shown in Fig. 1. However, to the best of our knowledge, there is no attempt to investigate local volume fraction effect of reinforced nanofillers inside polymer-based host materials through the multiscale modeling and analysis. In previous studies (Cho *et al*. 2011, and Shin *et al*. 2013), every interphase elastic properties are determined by global volume fraction and their particulate radii for dilute systems. In other words, few previous studies considered the contribution of local volume fraction effect. Therefore, in this study, we investigated the contribution of local volume fraction effect on the homogenized elastic properties.

Specifically, we performed multiscale analysis to investigate the contribution of overall volume fraction and the degree of local variations of nanoparticulate radii. For simplification of defining local volume fraction of nanofillers, nanoparticles are regularly arrayed in the host materials where the particulate radii are randomly distributed. To characterize these influences quantitatively, some parametric studies are mainly conducted about overall volume fraction of nanoparticles and local variation of radii between adjacent two nanoparticles. Extension to the multi-particulate system including nanoparticles which have regular array is conducted as well. Filler agglomeration is not main target of this study.

2. Review of multiscale modeling for polymer nanocomposites

2.1 Review of two-scale homogenization

Multiscale homogenization method is widely used to describe the mechanical deformation of macroscopic structure having periodic microstructures (Bendsøe *et al*. 1988, and Guedes *et al*. 1990). To describe both macroscopic and microscopic deformation behavior effectively, two scale coordinates are introduced where macroscopic coordinate and microscopic coordinate are denoted as **x** and **y**, respectively. Then, deformation field of overall domain could be described by the following form

$$\mathbf{u}(\mathbf{x},\mathbf{y}) = \mathbf{u}_0 + \mathbf{u}_1\varepsilon + \mathbf{u}_2\varepsilon^2 + \cdots \tag{1}$$

where the scale parameter ε is defined as $|\mathbf{x}|/|\mathbf{y}|$. Overall strain field could be obtained by differentiation of global coordinate as follows

$$
\begin{aligned}
u_{k,l} &= \frac{d}{dX_l}u_k = \left(\frac{d}{dx_l} + \frac{1}{\varepsilon}\frac{d}{dy_l}\right)\left(u_k^0 + u_k^1\varepsilon + u_k^2\varepsilon^2 + \cdots\right) \\
&= \varepsilon^{-1}\left(\frac{du_k^0}{dy_l}\right) + \varepsilon^0\left(\frac{du_k^0}{dx_l} + \frac{du_k^1}{dy_l}\right) + \varepsilon^1\left(\frac{du_k^1}{dx_l} + \frac{du_k^2}{dy_l}\right) + \cdots
\end{aligned}
\tag{2}
$$

For linear elasticity problem, constitutive equation and equilibrium equation are given as following forms

$$\sigma_{ij}(\mathbf{x},\mathbf{y}) = C_{ijkl}(\mathbf{y})u_{k,l}(\mathbf{x},\mathbf{y}) \tag{3a}$$

$$\frac{\partial \sigma_{ij}}{\partial x_j} + f_i = 0 \tag{3b}$$

By applying overall strain field and constitutive equation to the force equilibrium equation, the force equilibrium equation could be expanded as the following form

$$\varepsilon^{-2} : \frac{\partial \sigma_{ij}^{(0)}}{\partial y_j} = 0 \tag{4a}$$

$$\varepsilon^{-1} : \frac{\partial \sigma_{ij}^{(0)}}{\partial x_j} + \frac{\partial \sigma_{ij}^{(1)}}{\partial y_j} = 0 \tag{4b}$$

$$\varepsilon^{0} : \frac{\partial \sigma_{ij}^{(1)}}{\partial x_j} + \frac{\partial \sigma_{ij}^{(2)}}{\partial y_j} + f_i = 0 \tag{4c}$$

$$\varepsilon^{s-1} : \frac{\partial \sigma_{ij}^{(s)}}{\partial x_j} + \frac{\partial \sigma_{ij}^{(s+1)}}{\partial y_j} = 0 \tag{4d}$$

where Eq. (4b) is the microscopic equilibrium equation. Eq. (4b) could be computed by Eq. (5)

$$\frac{\partial}{\partial y_i}\left(C_{ijkl} - C_{ijmn}\frac{\partial \chi_k^{mn}}{\partial y_l} \right) = 0 \tag{5}$$

where microscopic displacement field $u_k^{(1)}(\mathbf{x}, \mathbf{y})$ is multiplicatively decoupled by the characteristic function $\chi_k^{mn}(\mathbf{y})$ and macroscopic strain field $\dfrac{\partial u_m^{(0)}(\mathbf{x})}{\partial x_n}$ as follows

$$u_k^{(1)}(\mathbf{x}, \mathbf{y}) = -\chi_k^{mn}(\mathbf{y})\frac{\partial u_m^{(0)}(\mathbf{x})}{\partial x_n} \tag{6}$$

The homogenized elastic stiffness tensor C_{ijkl}^{H} is obtained by the following form

$$C_{ijkl}^{H} = \frac{1}{|Y|}\int_Y C_{ijkl} - C_{ijmn}\frac{\partial \chi_k^{mn}}{\partial y_l} dV_y \tag{7}$$

where Y is the unit cell domain. Through finite element computation of Eqs. (5) and (7) with periodic boundary conditions, the homogenized elastic stiffness tensor is obtained in this study.

2.2 Characterization of the interfacial properties

2.2.1 Unit cell models of nanocomposites

The molecular models of nanocomposites having a single spherical silica (α-quartz) nanoparticles and polyimide as the reinforcing filler and matrix, respectively, were employed to
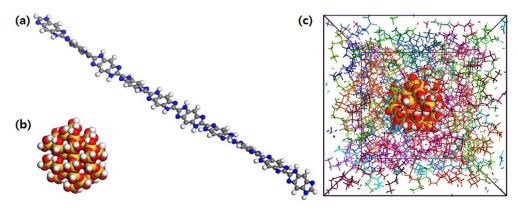
Fig. 2 Molecular modeling: (a) Nylon6 polymer chain (12 repeat units), (b) spherical silica (SiO$_2$) nanoparticle, and (c) polymer nanocomposites (LVN4)

Table 1 Unit-cell composition and elastic modulus of nanocomposites with a particulate volume fraction of 3% (Yang and Cho 2008)

Case	nanoparticulate radius (Å)	Cell length (Å)	Volume fraction (%)	*E* (GPa)	*G* (GPa)
LVN1	5.60	29.07	3	3.81	1.37
LVN2	6.16	31.99	3	3.39	1.26
LVN3	7.05	36.62	3	3.12	1.14
LVN4	8.36	43.42	3	2.89	1.04
LVN5	8.89	46.14	3	2.76	1.00

Table 2 Unit-cell composition and elastic modulus of nanocomposites with a particulate volume fraction of12% (Yang and Cho 2009)

Case	nanoparticulate radius (Å)	Cell length (Å)	Volume fraction (%)	*E* (GPa)	*G* (GPa)
HVN1	9.97	32.64	12	4.66	1.74
HVN2	10.74	35.16	12	4.20	1.54
HVN3	11.41	37.36	12	3.99	1.45
HVN4	12.01	39.32	12	3.81	1.38
HVN5	12.56	41.04	12	3.60	1.30

Table 3 Unit-cell composition and elastic modulus of nanocomposites with a particulate radius of 9.97 Å (Yang and Cho 2009)

Case	nanoparticulate radius (Å)	Cell length (Å)	Volume fraction (%)	*E* (GPa)	*G* (GPa)
DVN1	9.97	29.07	10	4.28	1.57
DVN2	9.97	31.99	8.5	3.62	1.32
DVN3	9.97	36.62	7.5	3.20	1.16
DVN4	9.97	43.42	6.5	3.36	1.22
DVN5	9.97	46.14	6.0	3.10	1.12

characterize the influence of filler size and volume fraction on the effective elastic properties in the previous study (Cho *et al*. 2011). In MD simulations, the unit cell structures were modeled as amorphous structures with periodic boundary conditions and a spherical silica nanoparticle is embedded at the center of the unit cell as shown in Fig. 2. During the determination of the radii of nanoparticles, an atomic diameter is not considered.

Details of the compositions of nanocomposites considered in the MD simulations are listed in Tables 1-3. In order to investigate the influence of nanofiller volume fraction and reinforced particulate radius on the elastic behavior of nanocomposites and effective interphase, the sets in Tables 1-3 are denoted as low volume fraction nanocomposites (LVN) (Yang and Cho 2008), high volume fraction nanocomposites (HVN) (Yang and Cho 2009), and differentiated volume fraction nanocomposites (DVN) (Yang and Cho 2009), respectively.

The number of polyimide chain is 12 repeat units in the set LVN and 10 repeat units in the set HVN and DVN. For every molecular dynamics modeling and simulation, Materials Studio 5.5.3® is employed, and COMPASS forcefield was used to describe the inter- and intra-atomic interactions. After constructing the initial amorphous structures, the potential energy of the unit cells were minimized via the conjugate gradient method. After energy minimization, conventional relaxation procedure for polymeric MD simulation (900 ps of NPT ensemble simulation at 300 K and 1 atm) is conducted to equilibrate the unit cells. The elastic stiffness tensor was calculated from the Parrinello-Rahman fluctuation method (Parrinello and Rahman 1982) with 10^4 strain fluctuation values after 600 ps of NσT ensemble simulation as follows

$$C_{ijkl} = \frac{k_B T}{\langle V \rangle} \left\langle \delta\varepsilon_{ij} \delta\varepsilon_{kl} \right\rangle^{-1} \tag{8}$$

where C_{ijkl} is elastic stiffness tensor, k_B is the Boltzmann constant, T, V, and $\delta\varepsilon$ are the temperature, volume, and strain tensor of the unit cell, respectively, and $\langle . \rangle$ is the ensemble average. In this study, interphase thickness was set to 5 Å for both dilute and non-dilute model (Cho *et al*. 2011). By radial density distribution of polymer phase, the interphase thickness was determined as 7 Å (Yang and Cho 2008). However, interphase is percolated due to periodic boundary condition at this interphase thickness, high volume fraction of 12 %, and low particulate radius. To avoid interphase percolated effect, the interphase thickness was set to 5 Å (Cho *et al*. 2011). Young's (shear) moduli of pure polyimide and spherical silica nanoparticle are 2.44 (0.88) GPa and 104 (37) GPa, respectively.

2.2.2 Numerical procedures to obtain the interfacial properties

The elastic stiffness tensor of the nanocomposites, matrix, and particles are obtained from MD simulation and reference data from experiments. To characterize interphase elastic properties, Cho *et al*. (2011) proposed numerical procedures by combining multiscale homogenization and MD simulation. The proposed numerical procedures are as follows

$$\text{error} = \sqrt{\left(\frac{E_{comp}^{MD} - E_{comp}^{H}(E_{int}, G_{int})}{E_{comp}^{MD}} \right)^2 + \left(\frac{G_{comp}^{MD} - G_{comp}^{H}(E_{int}, G_{int})}{G_{comp}^{MD}} \right)^2} \tag{9}$$

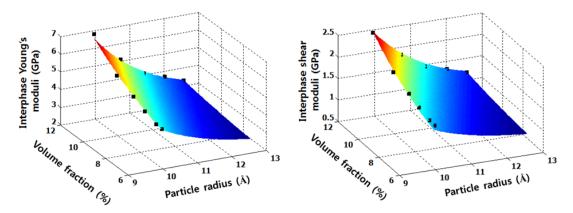where $E_{comp}^{MD}(G_{comp}^{MD})$ and $E_{comp}^{H}(G_{comp}^{H})$ are Young's(shear) moduli of nanocomposites obtained

Fig. 3 Interphase elastic properties obtained from the multiscale bridging method based on two-scale homogenization (solid square ■), and fitted surface as shown in Eq. (3a) and (3b) (3-D contours) for various particle radii and volume fraction: (a) Young's moduli, and (b) shear moduli

from MD simulation and multiscale homogenization, respectively, and $E_{int}(G_{int})$ are Young's(shear) moduli of effective interphase, respectively. The repetitive iteration steps are conducted until the error value in Eq. (2) reaches the error tolerance, 10^{-10}. Based on the nanocomposite elastic properties obtained from MD simulation, elastic properties of effective interphase were characterized. As a result, elastic properties of interphase were fitted into the functions of the particle radius and volume fraction as follows

$$E_{int}=2.44+276\exp(-2.95r_p/t_i+0.14f_p) \tag{10a}$$

$$G_{int}=0.88+80\exp(-3.05r_p/t_i+0.18f_p) \tag{10b}$$

where t_i is the thickness of the interphase and r_p is particulate radius (Cho *et al.* 2011).

Interphase elastic properties increase for decreasing particle radius and increasing volume fraction of reinforced filler as shown in Fig. 3. Elastic properties of interphase as function of filler radius and volume fraction have been already widely studied in previous works (Yang and Cho 2008, Yang and Cho 2009, Cho *et al.* 2011). Detail mechanical discussion on the tendency of interphase elastic properties are omitted in this study.

3. Numerical results and discussions

3.1 Influence of local variation of volume fraction

To investigate an influence of local volume fraction variation on the homogenized elastic properties, a number of finite element unit cell systems are constructed as shown in Table 4. For simplification, each unit cell system includes only two nanoparticles with interphase zone as shown in Fig. 4(a). In this study, numerical simulations are performed on the following two key parameters.

1. Overall volume fraction of nanoparticles
2. Deviation of local volume fractions between two nanoparticles

Table 4 Longitudinal elastic properties (E_L) of nanocomposites including two nanoparticles with different local volume fraction

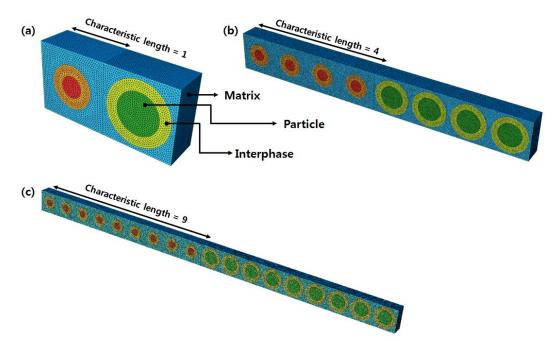| System	Volume fraction			Particulate radius (Å)			E_L of nanocomposites [GPa] w/ and w/o local volume fraction effect		
	Overall	A	B	$(r_p)_B/(r_p)_A$	A	B	w/	w/o	Deviation (%)
S01C1	3%	1.88%	4.12%	1.3	6.90	8.97	2.853	2.849	0.127%
S02C1	3%	1.18%	4.82%	1.6	5.91	9.46	2.842	2.831	0.387%
S03C1	3%	0.76%	5.24%	1.9	5.11	9.71	2.832	2.814	0.638%
S04C1	6%	3.75%	8.25%	1.3	6.90	8.97	3.647	3.610	1.019%
S05C1	6%	2.35%	9.65%	1.6	5.91	9.46	3.631	3.531	2.835%
S06C1	6%	1.53%	10.47%	1.9	5.11	9.71	3.613	3.462	4.363%
S07C1	10%	6.26%	13.74%	1.3	6.90	8.97	6.011	5.758	4.389%
S08C1	10%	3.92%	16.08%	1.6	5.91	9.46	6.038	5.401	11.779%
S09C1	10%	2.54%	17.46%	1.9	5.11	9.71	6.028	5.132	17.450%

Fig. 4 Representative volume element (RVE) including two types of nanoparticles with different characteristic length: (a) characteristic length: 1, (b) characteristic length: 4, and (c) characteristic length: 9

As shown in Table 4, the overall volume fractions of nanoparticles are selected as 3%, 6%, and 10% to investigate both dilute and non-dilute characteristics. To characterize an influence of local variation of volume fractions of two adjacent nanoparticles, the ratio of particulate radius between adjacent nanoparticles ($(r_p)_B / (r_p)_A$) is introduced and varied as 1.3, 1.6, and 1.9. For example, "S03C1" means that third system with one characteristic length where S and C denote system and
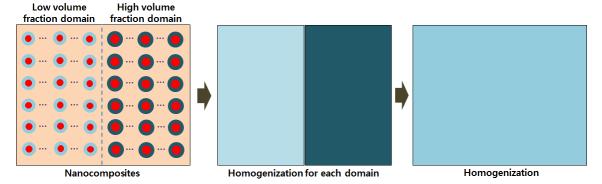
Fig. 5 Two-step homogenization process for large system including the infinite number of nanoparticles

characteristic length, respectively. As shown in Table 4, an influence of local volume fraction effect is non-negligible for the high volume fraction systems. The homogenized elastic properties without local volume fraction effect show the decreasing tendency. It is similar to the previous micromechanics studies considering filler agglomeration (Shi *et al*. 2004, Weng *et al*. 2011). As shown in Fig. 3, interphase elastic properties are very sensitive to the local volume fraction of nanoparticles when the local volume fraction is above 10 %. From this point, such sensitivity is critical at high overall volume fraction systems (S07C1, S08C1, and S09C1) where the local volume fractions of nanoparticles are above 10 %. For dilute model whose overall volume fraction is less than 6 %, local variation is not dominant factor as shown in Table 4. More specifically, the deviation of homogenization elastic properties (E_L) between the case whose local variation of volume fraction is considered and the case whose local variation of volume fraction is not considered is below only 1 %. However, for non-dilute model whose overall volume fraction is about 10 %, local variation shows non-negligible influence on the homogenized elastic properties (4-18% deviation) as shown in Table 4. In this regard, local variation effect should be considered to analyze high volume fraction systems such as the highlighted high volume fraction domain in Fig. 4(a). Meanwhile, local variation of volume fraction between two adjacent nanoparticles shows about four times increasing deviation for constant overall volume fraction of nanoparticles. As a result, an influence of such a local variation of volume fraction is critical in high volume fraction systems although this is negligible in low volume fraction systems.

3.2 Application on the large systems

In this section, unit cell including two nanoparticles is expanded to the large systems including the infinite number of nanoparticles. For extreme case, overall domain of unit cell could be divided into two domain of low volume fraction domain and high volume fraction domain as shown in Fig. 5. In Fig. 5, characteristic length is infinite. However, it is not practical to obtain such large systems. Therefore, in this section, three types of systems are constructed for various characteristic lengths. Convergence of homogenized elastic properties is verified for increasing characteristic length, and simple method to obtain the homogenization solution of large unit cell including the infinite number of nanoparticles is proposed as shown in Fig. 5.

In order to investigate convergence of homogenization results with respect to the increasing characteristic lengths, three types of systems are constructed for different characteristic lengths as

Table 5 Longitudinal elastic properties (E_L) of nanocomposites for various characteristic length

System	Volume fraction			Particulate radius (Å)			Characteristic length	E_L of nanocomposites [GPa] w/ and w/o local volume fraction effect	
	Overall	A	B	$(r_p)_B/(r_p)_A$	A	B		w/	w/o
S06C1 (Fig. 4(a))	6%	1.53%	10.47%	1.9	5.11	9.71	1	3.61	3.46
S06C4 (Fig. 4(b))	6%	1.53%	10.47%	1.9	5.11	9.71	4	3.59	3.44
S06C9 (Fig. 4(c))	6%	1.53%	10.47%	1.9	5.11	9.71	9	3.66	3.50
S06C∞ (Fig. 5)	6%	1.53%	10.47%	1.9	5.11	9.71	∞	3.65	3.49

shown in Fig. 4. In two-step homogenization process, each domain is homogenized through finite element homogenization of unit cell including single nanoparticles with interphase zone embedded in the center of cubic. After the homogenization of each domain, the homogenized elastic properties of overall domain are obtained from the homogenization of bi-domain including low volume fraction domain and high volume fraction domain. Some previous studies employ this schematic in order to obtain homogenized results of nanocomposite systems (Yang and Cho 2009, Friebel *et al*. 2006). Local fluctuations of interfacial traction and displacement condition between two adjacent domains are negligible because there is infinite number of nanoparticles near the interface.

As shown in Table 5, convergence of homogenized elastic properties is verified for increasing characteristic length. Homogenization results are almost not changed in spite of increasing characteristic length as shown in Table 5. Specifically, the proposed simple unit cells including only two nanoparticles with different local volume fraction shows similar homogenized elastic properties compared to the large systems of high characteristic length because the deviation is below 2 %. Therefore, simple unit cell including only two nanoparticles could represent the multi-particulate domain as shown in Fig. 5.

4. Conclusions

A multiscale analysis of homogenized elastic properties to investigate local volume fraction effect is conducted because interphase elastic properties are dependent on the volume fraction of reinforced nanoparticles. Parametric studies provide some insights described below:

• For high overall volume fraction systems, the local variation of volume fraction should be considered.

• To describe high volume fraction domain including cluster whose array is regular, consideration of only two nanoparticles is adequate.

The simulation results show that local volume fraction effect should be considered when the fillers have high variation of particulate radii, and randomly distributed. In future work, the local variation of volume fraction will be considered for multi-particulate systems including polydispersed nanoparticles.

Acknowledgements

References

Barai, P. and Weng, G.J. (2011), "A theory of plasticity for carbon nanotube reinforced composites", *Int. J. Plast.*, **27**(4), 539-559.

Bendsøe, M.P. and Kikuchi, N. (1988), "Generating optimal topologies in structural design using a homogenization method", *Comput. Method. Appl. Mech. Eng.*, **71**(2), 197-224.

Cho, M., Yang, S., Chang, S. and Yu, S. (2011), "A study on the prediction of the mechanical properties of nanoparticulate composites using the homogenization method with the effective interface concept", *Int. J. Numer. Meth. Eng.*, **85**(12), 1564-1583.

Friebel, C., Doghri, I. and Legat, V. (2006), "General mean-field homogenization schemes for viscoelastic composites containing multiple phases of coated inclusions", *Int. J. Solid. Struct.*, **43**(9), 2513-2541.

Goyal, R.K., Tiwari, A.N., Mulik, U.P. and Negi, Y.S. (2008), "Thermal expansion behavior of high performance PEEK matrix composites", *J. Phys. D: Appl. Phys.*, **41**(8), 085403.

Guedes, J.M. and Kikuchi, N. (1990), "Preprocessing and postprocessing for materials based on the homogenization method with adaptive finite element methods", *Comput. Method. Appl. Mech. Eng.*, **83**(2), 143-198.

Kim, B., Choi, J., Yang, S., Yu, S. and Cho, M. (2015), "Influence of crosslink density on the interfacial characteristics of epoxy nanocomposites", *Polymer*, **60**, 186-197.

Liu, J., Gao, Y., Cao, D., Zhang, L. and Guo, Z. (2011), "Nanoparticle dispersion and aggregation in polymer nanocomposite: Insights from molecular dynamics simulation", *Langmuir*, **27**(12), 7926-7933.

Odegard, G.M., Clancy, T.C. and Gates, T.S. (2005), "Modeling of the mechanical properties of nanoparticle/polymer composites", *Polymer*, **46**(2), 553-562.

Parrinello, M. and Rahman, A. (1982), "Strain fluctuations and elastic constants", *J. Chem. Phys.*, **76**(5), 2662-2666.

Shi, D.-L., Feng, X.-Q., Huang, Y. Y., Hwang, K.-C. and Gao, H. (2004), "The effect of nanotube waviness and agglomeration on the elastic property of carbon nanotube-reinforced composites", *Trans. ASME J. Appl. Mech.*, **126**(3), 250-257.

Shin, H., Yang, S., Chang, S., Yu, S. and Cho, M. (2013), "Multiscale homogenization modeling for thermal transport properties of polymer nanocomposites with Kapitza thermal resistance", *Polymer*, **54**(5), 1543-1554.

Thostenson, E.T., Li, C. and Chou, T.W. (2005), "Nanocomposites in context", *Compos. Sci. Technol.*, **65**(3), 491-516.

Vu-Bac, N., Lahmer, T., Keitel, H., Zhao, J., Zhuang, X. and Rabczuk, T. (2014), "Stochastic predictions of bulk properties of amorphous polyethylene based on molecular dynamics simulations", *Mech. Mater.*, **68**, 70-84.

Wei, C., Srivastava, D. and Cho, K. (2002), "Thermal expansion and diffusion coefficients of carbon nanotube-polymer composites", *Nano. Lett.*, **2**(6), 647-650.

Xu, N., Dai, J., Zhu, Z., Huang, X. and Wu, P. (2012), "Synthesis and characterization of hollow glass-ceramics microspheres", *Compos. Sci. Technol.*, **72**(4), 528-532.

Yang, S. and Cho, M. (2008), "Scale bridging method to characterize mechanical properties of nanoparticle/polymer nanocomposites", *Appl. Phys. Lett.*, **93**(4), 043111.

Yang, S. and Cho, M. (2009), "A scale-bridging method for nanoparticulate polymer nanocomposites and their nondilute concentration method", *Appl. Phys. Lett.*, **94**(22), 223104.

Yang, S., Choi, J. and Cho, M. (2012), "Elastic stiffness and filler size effect of covalently grafted nanosilica polyimide composites: molecular dynamics study", *ACS Appl. Mater. Interfaces.*, **4**(9), 4792-4799.

Yang, S., Yu, S., Kyoung, W., Han, D.-S. and Cho, M. (2012), "Multiscale modeling of size-dependent elastic properties of carbon nanotube/polymer nanocomposites with interfacial imperfections", *Polymer*, **53**(2), 623-633.

Zeng, Q.H., Yu, A.B. and Lu, G.Q. (2008), "Multiscale modeling and simulation of polymer nanocomposites", *Prog. Polym. Sci.*, **33**(2), 191-269.

MC